https://doi.org/10.33263/Materials22.097102

ISSN: 2668-5728 https://materials.international

Materials International

Volume 2, Issue 2, Pages 0097-0102
2020

Received: 09.03.2020
Accepted: 05.04.2020
Published: 13.04.2020

Article

Effects of Substrate Type on the Morphology and Optical Properties of ZnO Nanorods Grown via Chemical Bath Deposition

Yasmine Taha [1], Hanaa F. Al-Taay [1,*]

[1] Department of physics, College of science for Women, University of Baghdad, Baghdad, Iraq
* Correspondence: Hanaa_flayeh@yahoo.com; Scopus ID: 55331327200

Abstract: In this study, zinc oxide nanorods (ZnO NRs) were prepared through chemical bath deposition using glass and fluorine-doped tin oxide (FTO) substrates, and their crystalline structure was investigated through X-ray diffraction. Results showed that the prepared ZnO NRs had wurtzite structure and grew along the [002] orientation, and ZnO NRs grown on the FTO substrate was more crystalline than those grown on the glass substrate. Field-emission scanning electron microscopy images showed that the glass sample had rod-like morphology and uniform distribution with 95 nm diameter and average length of approximately 980 nm, whereas the FTO-coated glass had 110 nm diameter and average length of approximately 1000 nm. The direct transition optica1 band gaps of the glass and FTO-coated glass samples were 3.28 and 3.97 eV, respectively.

Keywords: Nanomaterial; ZnO Nanorods; CBD Method; Structure and Optical Properties.

1. Introduction

1D nanostructured semiconductors, such as nanowires, nanorods (NRs), nanoribbons, nanotubes, and nanosheets, are widely investigated because of their distinct physica1 and chemica1 properties [1]. These nanostructures are widely used in numerous technological app1ications [2,3]. Zinc oxide (ZnO) is a suitable nanomateria1 in nanotechnology [4]. ZnO is an important semiconductor materia1, and has unique properties, such as wide band gap of 3.37 eV at 300 K, high excitation energy of 60 meV at room temperature [5–8], environment friendly, chemica1ly stab1e, low cost, and easy synthesis in nanostructured forms [9–12]. It has been widely used in optoelectronic devices, piezoelectric devices, sensors, and solar cells [13–15]. 1D ZnO NRs have several unique advantages, including high crystallinity, high sensitivity to adsorbed oxygen on the surface, fie1d-emission, excellent e1ectron transport, optica1 wave guiding, and high surface area-to-vo1umeratio [16–18]. ZnO nanostructures can be synthesized using different methods, such as so1–ge1 [19], hydrothermal [8, 20], sputtering [21], pulsed laser deposition [8],spin coating [8)], chemica1 vapor deposition, [22], chemica1 bath deposition (CBD) [23], and others [9,24]. Among these techniques, CBD provides many advantages, such as low-temperature requirement, low cost, and can deposit thin fi1ms on different types of substrates.

Cite This Article: Taha, Y.; Al-Taay, H.F. Effects of Substrate Type on the Morphology and Optical Properties of ZnO Nanorods Grown via Chemical Bath Deposition. Mat Int **2020**, 2, 0097-0102. https://doi.org/10.33263/Materials22.097102

In the present study, ZnO NRs were prepared on fluorine-doped tin oxide (FTO)-coated glass and glass substrates, and their applications were studied.

2. Materials and Methods

All chemicals were of analytica1 grade and used without purification. ZnO NRs were successively prepared through the spin coating and CBD. Glass and FTO-coated glass substrates were successively c1eaned using an u1trasonic bath in 2-propanol, acetone, and deionized (DI) water for 20 min and then dried at 60 °C.

The seed layer of ZnO was prepared through spin coating. Zinc acetate [$ZnC_4H_6O_4$; 0.005 M] was dissolved in pure ethanol at room temperature. The solution was continuously stirred for 1 h at 60 °C using a magnetic stirrer to obtain a transparent and homogeneous so1 and stored for one day.

The two substrates were spin-coated with the so1 and heated at 100 °C for 10 min. This process was repeated thrice. The seed 1ayer was annea1ed in a tube furnace at 300 °C for 1 h.

Precursor aqueous solution of 0.004 M zinc nitrate hexahydrate [$ZnO(NO_3)_{26}H_2O$] and 0.0025 M hexamethylenetetramine [$C_6H_{12}N_4$] (HMT) were prepared to grow ZnO NRs. ZnO NRs on the glass and FTO-coated glass substrate-seeded substrates were immersed in the precursor so1ution and magnetically stirred at 90 °C for 2 h. After the comp1etion of growth, the substrates were c1eaned with DI water and annea1ed at 300 °C for 1 h.

3. Results and Discussion

3.1. Structure of ZnO

Figure 1 shows the X-ray diffraction (XRD) patterns of the ZnO seed layer deposited on glass and FTO-coated glass substrates measured using an X–ray diffractometer with CuKα λ of 1.5406 Å at the scan range (2θ) of 10°–70°. The diffraction peaks recorded at 2θ values can be indexed to the different planes of crystalline ZnO with wurtzite structure and agrree with the standard (JCPDS 36-1451). Three sharp peaks are observed in the two substrates, which is consistent with the ZnO films with hexagonal wurtzite structure. The sharp peaks at (100), (002), and (101) of the aligned ZnO NRs have good crystallite structures. Karak et al. [25], Alarabi et al. [26], Jitao Li1 et al. (14), W. Li et al. [7] and Kumar et al. [27] prepared ZnO NRs using different methods, and they found that the peak level (002) is the highest.

3.2. Surface morphology of ZnO

Figure 2(A) shows the field-emission scanning electron microscopy (FE-SEM images) of the prepared ZnO nanocrystalline thin-films on the glass substrates through spin coating. These thin films exhibit a random distribution of ZnO nanoparticles with a diameter ranging from 15 nm to 22 nm. Figure 2(B) shows the ZnO NRs prepared on the FTO-coated glass substrates using the same method. These ZnO NRs have a diameter ranging from 31 nm to 48 nm and are composed of dense and uniform particles with neighboring particles connected together on the FTO substrate. Figure 2(C) illustrates the ZnO NRs prepared on glass through CBD. These NRs have asymmetrically distributed hexagonal-shaped ZnO particles with rod-like morphology. The asymmetric characteristic of ZnO rods can be because of the random distribution on the surface of the seed 1ayer of ZnO crystallites. Figure 2(D) shows the ZnO NRs prepared through CBD on the FTO seed layer culminated in vertically aligned hexagonal ZnO NRs with a diameter of 40–280 nm. Kumar et al. [27] prepared ZnO NRs using low-temperature solution growth techniques and obtained ZnO NRs with hexagonal shape.

The diameter ,distribution was calculated, as shown in Figure 3. As shown in Figure 3(A), the diameter of ZnO NRs on the glass substrate ranged from 30 nm to 120 nm, and the average diameter was 95 nm. As shown in Figure 3(B), the diameter of ZnO NRs prepared on FTO substrate ranged from 40 nm to 260 nm, and the average diameter was 110 nm. The rod densities of ZnO NRs on, the

glass and 0FTO-coated0 glass substrates were 62 and 32 NR/μm^2, respectively.

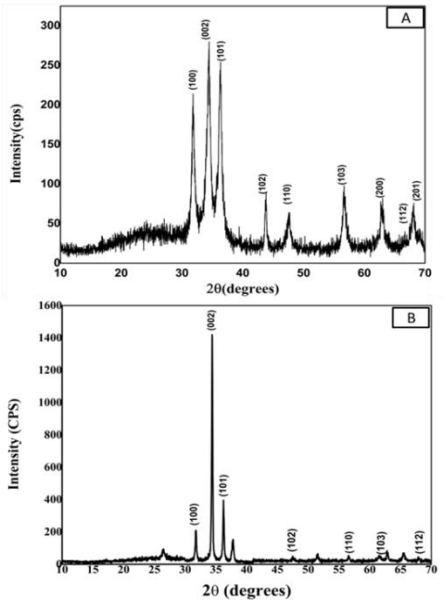

Figure 1. XRD patterns of ZnO NRs on (A) glass and (B) FTO-coated glass substrates.

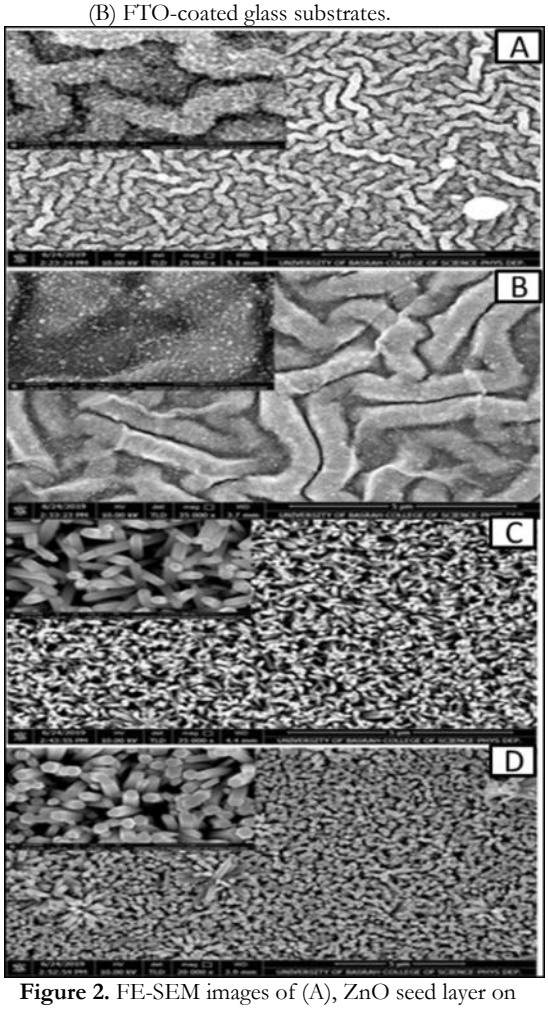

Figure 2. FE-SEM images of (A), ZnO seed layer on glass- substrate, (B) ZnO seed layer on FTO-coated, glass, substrate, (C) ZnO NRs, grown on glass substrate, and (D) ZnO NRs grown on FTO-coated glass.

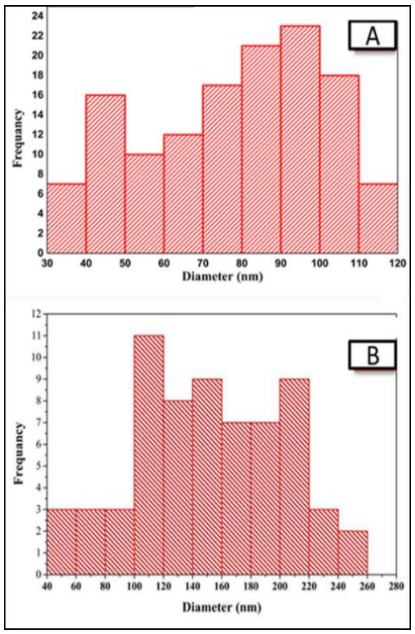

Figure 3. Diameter distribution of the ZnO NRs grown on the (A) glass and (B) FTO-coated glass substrates.

The cross-sectiona1 SEM s of the grown ZnO NRs are shown in Figure 4. The ZnO NRs developed densely on the FTO-coated glass substrate with uniform morphology. The average length of the ZnO NRs was 1000 nm. ZnO NRs were successfully grown and covered the FTO-coated glass substrate. The ZnO NRs on the glass substrate had an average length of 980 nm. However, The avarage diameter , density and average length of prepared ZnO NRs grown on glass and FTO –coated glass substrates are listed in Tabel 1.

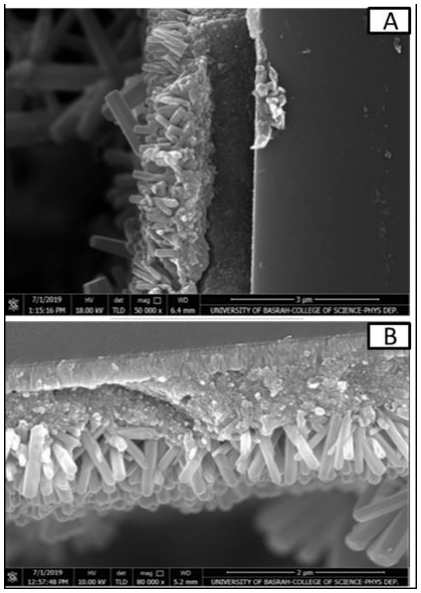

Figure 4. Cross-sectional SEM images of ZnO NRs on the (A) glass and (B) FTO-coated glass substrates.

Table 1. The Average diameter , Density and Average length of ZnO NRs grown on glass and FTO –coated glass substrates were calculated from morphology examination.

	Glass substrate	FTO_coated glass substrate
Avarge diameter (nm)	95	110
Density (NR/μm²)	62	32
Avrage length(nm)	980	1000

3.3. Optical properties of ZnO.

The absorption behavior of ZnO NRs was studied by analyzing the ultraviolet–visible (UV–vis) spectra. The typica1 UV–vis spectra of the ZnO thin-film are shown in Figure 5. Optica1 absorbance edge appeared at around (367nm), and (370nm) was observed on the glass and FTO-coated glass substrates, respectively. The band gap of the ZnO thin film was ca1cu1ated from the absorption spectra using the Tauc equation as follows [28]:

$$hv = D(hv - Eg)^{\wedge}n \qquad (1)$$

where h is the energy of the photon, Eg is the band gap of the material, and D is a constant. The transition data provide the best linear fit for n = 1/2 in the band edge region. The plot of $(hν)^2$ versus hν is shown in Figure 6. The bandgap was ca1culated by extrapo1ating the 1inear portion of the p1ot on the hν axis in the high absorption region and found to be 3.28 eV for the glass substrate, which is smaller than that of the bulk ZnO (3.37 eV). This band gap enhancement is because of the size effect of the nanoparticles in the thin fi1m. The FTO-coated glass had a band gap of 3.97 eV, which is consistent with the Eg value reported by Ocakoglu (3) and Ghoshal (18) in their investigation of ZnO NRs synthesized through CBD.

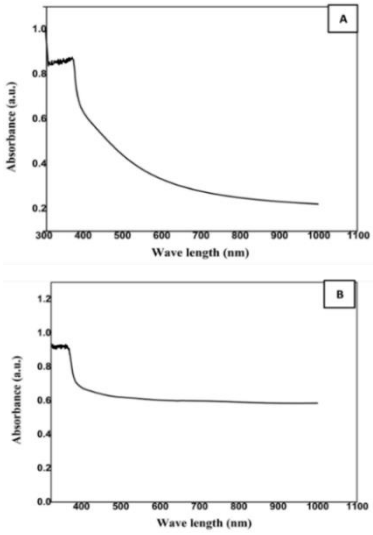

Figure 5. UV–vis spectra of the ZnO NRs on the (A) glass and (B) FTO-coated glass substrates.

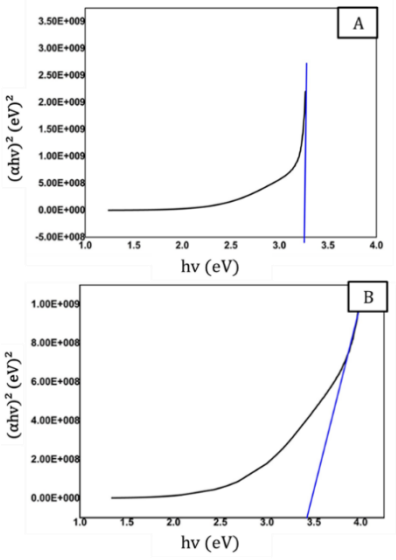

Figure 6. Tauc plot for the band gap determination of ZnO NRs on the (A) glass and (B) FTO-coated glass substrates.

4. Conclusions

In this study, ZnO NRs were prepared through CBD, and their surface morphology, optical, and structural properties were investigated. The ZnO seed layer was prepared on well-cleaned glass and FTO-coated glass substrates through CBD. The ZnO seed substrates were immersed in aqueous zinc nitrate solution and HMT at 90 °C for 2 h. The XRD results showed that the ZnO NRs have three sharp peaks at (100), (002), and (101), with (002) as the preferred orientation. The band gaps of the prepared ZnO NRs were calculated and were found to be 3.28 and 3.97 eV for the glass and FTO-coated glass substrates, respectively. The SEMimages show that the ZnO NRs grown on the glass substrate have 95 nm diameter and 980 nm length, whereas the ZnO NRs grown on the FTO-coated glass substrate have 110 nm diameter and 1000 nm length. The ZnO NRs grown on different substrates are suitable to be used in different optoelectronic devices, particularly in

improving organic solar cells, because of their optical characteristics.

Funding
This research received no external funding.

Acknowledgments
The authors declare no acknowledgments.

Conflicts of Interest
The authors declare no conflict of interest.

References

1. Abdul-Hameed, A.A; Ali, B.; Al-Taay, H.F.; Mahdi, M.A. Fabrication of SiNWs/PEDOT:PSS Heterojunction Solar Cells, *Iranian Journal of Materials Science & Engineering* **2020**, *17*, 69-76, https://doi.org/10.22068/ijmse.17.1.69
2. Al-Taay, H.F.; Mahdi, M.A.; Parlevliet, D.; Jennings, P. Controlling the diameter of silicon nanowires grown using a tin catalyst. *Materials Science in Semiconductor Processing* **2013**, *16*, 15-22, https://doi.org/10.1016/j.mssp.2012.07.006.
3. Al-Taay, H.F.; Mahdi, M.A.; Parlevliet, D.; Hassan, Z.; Jennings, P. Growth and characterization of silicon nanowires catalyzed by Zn metal via Pulsed Plasma-Enhanced Chemical Vapor Deposition. *Superlattices and Microstructures* **2014**, *68*, 90-100, https://doi.org/10.1016/j.spmi.2014.01.014.
4. Chey, C.O.; Alnoor, H.; Abbasi, M.A.; Nur, O.; Willander, M. Fast synthesis, morphology transformation, structural and optical properties of ZnO nanorods grown by seed-free hydrothermal method. *physica status solidi (a)* **2014**, *211*, 2611-2615, https://doi.org/10.1002/pssa.201431311.
5. Tiwari, R.A.; Narayan, J. Electrical properties of transparent and conducting Ga doped ZnO. *Journal of Applied Physics* **2006**, *100*, https://doi.org/10.1063/1.2218466.
6. Boukhoubza, I.; Khenfouch, M.; Achehboune, M.; Mothudi, B.M.; Zorkani, I.; Jorio, A. Graphene oxide/ZnO nanorods/graphene oxide sandwich structure: The origins and mechanisms of photoluminescence. *Journal of Alloys and Compounds* **2019**, *797*, 1320-1326, https://doi.org/10.1016/j.jallcom.2019.04.266.
7. Li, W.; Guo, Y.J.; Tang, Q.B.; Zu, X.T.; Ma, J.Y.; Wang, L.; Tao, K.; Torun, H.; Fu, Y.Q. Highly sensitive ultraviolet sensor based on ZnO nanorod film deposited on ST-cut quartz surface acoustic wave devices. *Surface and Coatings Technology* **2019**, *363*, 419-425, https://doi.org/10.1016/j.surfcoat.2019.02.041.
8. Hassan, A.; Jin, Y.; Azam, M.; Irfan, M.; Jiang, Y. Large photoluminescence enhancement in mechanical-exfoliated one-dimensional ZnO nanorods. *Journal of Materials Science: Materials in Electronics* **2019**, *30*, 5170-5176, http://dx.doi.org/10.1007/s10854-019-00815-1.
9. Ocakoglu, K.; Mansour, S.A.; Yildirimcan, S.; Al-Ghamdi, A.A.; El-Tantawy, F.; Yakuphanoglu, F. Microwave-assisted hydrothermal synthesis and characterization of ZnO nanorods. *Spectrochimica Acta Part A: Molecular and Biomolecular Spectroscopy* **2015**, *148*, 362-368, https://doi.org/10.1016/j.saa.2015.03.106.
10. Santoshkumar, B.; Kalyanaraman, S.; Vettumperumal, R.; Thangavel, R.; Kityk, I.V.; Velumani, S. Structure-dependent anisotropy of the photoinduced optical nonlinearity in calcium doped ZnO nanorods grown by low cost hydrothermal method for photonic device applications. *Journal of Alloys and Compounds* **2016**, *658*, 435-439, https://doi.org/10.1016/j.jallcom.2015.10.067.
11. Hassan, J.J.; Mahdi, M.A.; Chin, C.W.; Abu-Hassana, H.; Hassan, Z. Room temperature hydrogen gas sensor based on ZnO nanorod arrays grown on a SiO2/Si substrate via a microwave-assisted chemical solution method, *Journal of Alloys and Compounds* **2013**, 546, 107-111, https://doi.org/10.1016/j.jallcom.2012.08.040
12. Anand, A.; Bhatnagar, M.C. Role of vertically aligned and randomly placed zinc oxide (ZnO) nanorods in PVDF matrix: Used for energy harvesting. *Materials Today Energy* **2019**, *13*, 293-301, https://doi.org/10.1016/j.mtener.2019.06.005.
13. Lv, J.; Yan, P.; Zhao, M.; Sun, Y.; Shang, F.; He, G.; Zhang, M.; Sun, Z. Effect of ammonia on morphology, wettability and photoresponse of ZnO nanorods grown by hydrothermal method. *Journal of Alloys and Compounds* **2015**, *648*, 676-680, https://doi.org/10.1016/j.jallcom.2015.07.068.
14. Li, J.; Zhang, Y.; Zhang, Z.; Tian, Z. Facile Synthesis of ZnO Nanorods/GO Composite and Its Optical Performance. *J Nanosci Nanotechnol* **2019**, *19*, 2379-2384, https://doi.org/10.1166/jnn.2019.16483.
15. Viter, R.; Savchuk, M.; Starodub, N.; Balevicius, Z.; Tumenas, S.; Ramanaviciene, A.; Jevdokimovs, D.; Erts, D.; Iatsunskyi, I.; Ramanavicius, A. Photoluminescence immunosensor based on bovine leukemia virus proteins immobilized on the ZnO nanorods. *Sensors and Actuators B: Chemical* **2019**, *285*, 601-606, https://doi.org/10.1016/j.snb.2019.01.054.
16. Hassan, J.J.; Mahdi, M.A.; Ramizy, A.; Abu

Hassan, H.; Hassan, Z. Fabrication and characterization of ZnO nanorods/p-6H–SiC heterojunction LED by microwave-assisted chemical bath deposition. *Superlattices and Microstructures* **2013**, *53*, 31-38, https://doi.org/10.1016/j.spmi.2012.09.013.

17. Roza, L.; Fauzia, V.; Abd. Rahman, M.Y.; Jurusan, A.; Fisika, P.; Keguruan, F.; Pendidikan, I.; Muhammadiyah, U.; Hamka, J.; Timur, I. Tailoring the active surface sites of ZnO nanorods on the glass substrate for photocatalytic activity enhancement. Surfaces and Interfaces **2019,** *15,* https://doi.org/10.1016/j.surfin.2019.02.009.

18. Wahab, R.; Ahmad, N.; Alam, M.; Ahmad, J. Nanorods of ZnO: An effective hydrazine sensor and their chemical properties. *Vacuum* **2019**, *165*, 290-296, https://doi.org/10.1016/j.vacuum.2019.04.036.

19. Addonizio, M.L.; Aronne, A.; Daliento, S.; Tari, O.; Fanelli, E.; Pernice, P. Sol–gel synthesis of ZnO transparent conductive films: The role of pH. *Applied Surface Science* **2014**, *305*, 194-202, https://doi.org/10.1016/j.apsusc.2014.03.037.

20. Baruah, S.; Dutta, J. pH-dependent growth of zinc oxide nanorods. *Journal of Crystal Growth* **2009**, *311*, 2549-2554, https://doi.org/10.1016/j.jcrysgro.2009.01.135.

21. Manouchehri, I.; Gholami, K.; Astinchap, B.; Mordian, R.; Mehrparvar, D. Investigation of annealing effects on optical properties of Ti thin films deposited by RF magnetron sputtering. *Optik* **2016**, *127*, 5383-5389, https://doi.org/10.1016/j.ijleo.2016.03.013.

22. Meléndrez, M.F.; Solis-Pomar, F.; Gutierrez-Lazos, C.D.; Flores, P.; Jaramillo, A.F.; Fundora, A.; Pérez-Tijerina, E. A new synthesis route of ZnO nanonails via microwave plasma-assisted chemical vapor deposition. *Ceramics International* **2016**, *42*, 1160-1168, https://doi.org/10.1016/j.ceramint.2015.09.046.

23. Peng, W.; Qu, S.; Cong, G.; Wang, Z. Synthesis and Structures of Morphology-Controlled ZnO Nano- and Microcrystals. *Crystal Growth & Design* **2006**, *6*, 1518-1522, https://doi.org/10.1021/cg0505261.

24. Polsongkram, D.; Chamninok, P.; Pukird, S.; Chow, L.; Lupan, O.; Chai, G.; Khallaf, H.; Park, S.; Schulte, A. Effect of synthesis conditions on the growth of ZnO nanorods via hydrothermal method. *Physica B: Condensed Matter* **2008**, *403*, 3713-3717, https://doi.org/10.1016/j.physb.2008.06.020.

25. Karak, N.; Samanta, P.K.; Kundu, T.K. Green photoluminescence from highly oriented ZnO thin film forphotovoltaic application. *Optik (Stuttg)* **2013**, *124*, 6227–30, http://dx.doi.org/10.1016/j.ijleo.2013.05.019.

26. Alarabi, A.; Zeng, Z.; Gao, Y.; Gao, S.; Jiao, S.; Wang, D.; Wang, J. Influence of different substrates on ZnO nanorod arrays properties. *Solid State Sciences* **2018**, *85*, 21-25, https://doi.org/10.1016/j.solidstatesciences.2018.09.004.

27. Kumar, R.S.; Sudhagar, P.; Matheswaran, P.; Sathyamoorthy, R.; Kang, Y.S. Influence of seed layer treatment on ZnO growth morphology and their device performance in dye-sensitized solar cells. *Materials Science and Engineering: B* **2010**, *172*, 283-288, https://doi.org/10.1016/j.mseb.2010.05.032.

28. Selmana, A.M.; Mahdi, M.A.; Hassan, Z. Fabrication of Cu2O nanocrystalline thin films photosensor prepared by RF sputtering technique, *Physica E: Low-dimensional Systems and Nanostructures* **2017**, *94*, 132-138 https://doi.org/10.1016/j.physe.2017.08.007